



Cite this: *Dalton Trans.*, 2015, **44**, 6340

Received 2nd February 2015,

Accepted 5th March 2015

DOI: 10.1039/c5dt00481k

www.rsc.org/dalton

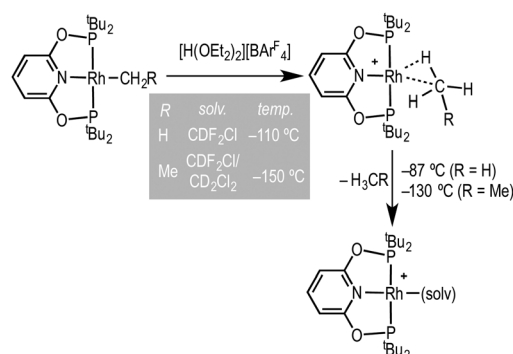
A CH₂Cl₂ complex of a [Rh(pincer)]⁺ cation†

Gemma M. Adams, F. Mark Chadwick, Sebastian D. Pike and Andrew S. Weller*

The CH₂Cl₂ complex [Rh(^tBuPONOP)(κ¹-ClCH₂Cl)][BAR^F₄] is reported, that also acts as a useful synthon for other complexes such as N₂, CO and H₂ adducts; while the analogous PNP complex undergoes C–Cl activation.

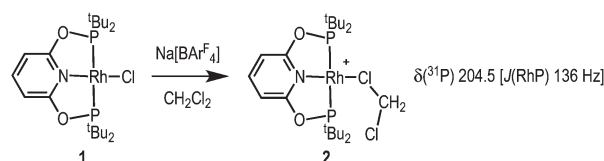
Coordinatively and electronically unsaturated transition-metal pincer complexes, [M(pincer)], are key intermediates in alkane dehydrogenation processes,¹ as well as other catalytic transformations.² They have also played a major role in the elucidation of fundamental bond transformations, such as C–H, C–C and C–X breaking and making.³ Recently, Brookhart and co-workers reported the synthesis of transition-metal methane and ethane sigma complexes, by a low temperature (*ca.* –110 °C to –150 °C) protonation of the corresponding Rh(^tBuPONOP)R precursors using [H(OEt)₂][BAR^F₄] in CDF₂Cl–CH₂Cl₂ solvent to give [Rh(^tBuPONOP)(H–R)][BAR^F₄] [^tBuPONOP = 2,6-(^tBu₂PO)₂C₅H₃N; R = Me, Et; Ar^F = 3,5-(CF₃)₂C₆H₃], Scheme 1.⁴ Such complexes are key, but transient, intermediates in C–H bond activation processes. On warming above –87 °C (R = Me) or –130 °C (R = Et) they lose alkane and generate complexes tentatively characterised *in situ* on the basis of ³¹P NMR spectroscopy as [Rh(^tBuPONOP)(solv)][BAR^F₄] (solv = CDF₂Cl or CD₂Cl₂). These solvent adducts remain to be definitively characterised. They are particularly interesting given their role in alkane coordination chemistry, and more generally as latent-low coordinate intermediates in catalytic processes.

We now report the full characterisation of the CH₂Cl₂ adduct accessed *via* a different, halide abstraction, route including a single crystal X-ray diffraction study and its onward reactivity. We also demonstrate that changing the pincer ligand to the more electron donating ^tBuPNP [2,6-(^tBu₂PCH₂)₂C₅H₃N] results in C–Cl bond activation of the solvent molecule.



Scheme 1 Formation of a sigma alkane complex and decomposition to give tentatively characterised solvent complexes (Brookhart and co-workers). [BAR^F₄][–] anions are not shown.⁴

Addition of Na[BAR^F₄] to a CH₂Cl₂ solution of Rh(^tBuPONOP)Cl, **1**,^{4a} results in the formation of orange [Rh(^tBuPONOP)(κ¹-ClCH₂Cl)][BAR^F₄], **2** (Scheme 2). Filtration and removal of the solvent affords **2** in good isolated yield as a powder. Complex **2** can be recrystallised from CH₂Cl₂–pentane under an Ar atmosphere to give crystals suitable for an X-ray diffraction study. Under these conditions, orange **2** crystallises alongside the dinitrogen adduct, [Rh(^tBuPONOP)(κ¹-N₂)][BAR^F₄], **3**, in an approximate 1 : 1 ratio (as measured by ³¹P NMR spectroscopy, *vide infra*). Single crystals of **2** suitable for an X-ray diffraction study were obtained by mechanical separation from orange/brown **3**.[‡] Presumably the exogenous N₂ comes from trace (1–2 ppm) levels of N₂ present in the argon, as has been noted previously,⁵ and is driven by relative solubilities of



Scheme 2 Synthesis of complex **2**. [BAR^F₄][–] anion is not shown.

Department of Chemistry, Chemistry Research Laboratories, Mansfield Road, Oxford, OX1 3TA, UK. E-mail: andrew.weller@chem.ox.ac.uk

†Electronic supplementary information (ESI) available: Full experimental, characterisation and X-ray crystallography details. CCDC 1044741, 1044743, 1044744 and 1044745. For ESI and crystallographic data in CIF or other electronic format see DOI: 10.1039/c5dt00481k



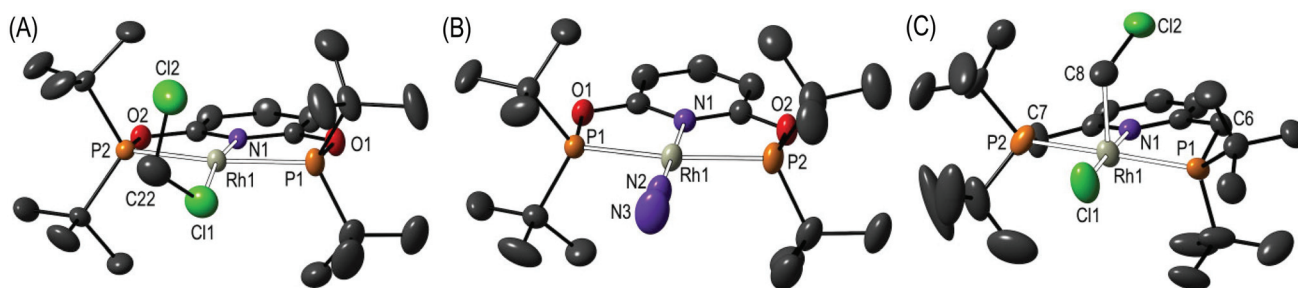


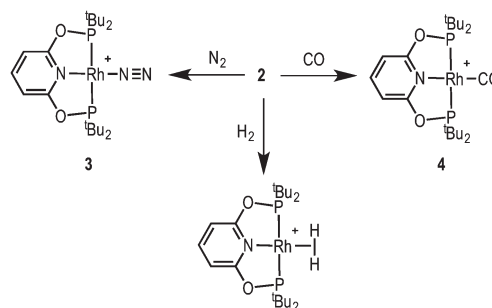
Fig. 1 Solid-state structures of: (A) Complex 2; (B) Complex 3; (C) Complex 5. Displacement ellipsoids are shown at the 50% probability level, hydrogen atoms and the $[\text{BARF}_4]^-$ anions are not shown. Selected bond lengths (\AA) and angles ($^\circ$): (2) Rh1–Cl1, 2.350(2); Rh1–N1, 2.011(4); Rh1–P1, 2.272(1); Rh1–P2, 2.285(1); Cl1–C22, 1.710(8); Cl2–C22, 1.758(7); Cl1–C22–Cl2, 114.3(4); N1–Rh1–Cl1, 169.65(11). (3) Rh1–N1, 2.018(3); Rh1–N2, 1.967(3); Rh1–P1, 2.2745(8); Rh1–P2, 2.2724(8); N2–N3, 1.063(5); Rh1–N2–N3, 179.3(4); N1–Rh1–N2, 179.37(13). (5) Rh1–Cl1, 2.311(2); Rh1–N1, 2.066(6); Rh1–P1, 2.335(2); Rh1–P2, 2.339(2); Rh1–C8, 2.196(15); C8–Cl2, 1.79(2); Rh1–C8–Cl2, 112.5(9). Complex 5 co-crystallises with $[\text{Rh}(\text{tBuPnP})(\text{H})\text{Cl}][\text{BARF}_4]$, **6**, at the same lattice position in a 50 : 50 ratio.†

2 and **3**; as in neat CD_2Cl_2 under the same Ar atmosphere **2** does not go on to form **3** to the detection limit of $^{31}\text{P}\{^1\text{H}\}$ NMR spectroscopy. The solid-state structure (Fig. 1A) shows a pseudo square planar cationic $[\text{Rh}(\text{tBuPONOP})]^+$ centre coordinated in the fourth position by a CH_2Cl_2 molecule. The Rh–Cl1 distance [2.350(2) \AA] is significantly shorter than reported for related $[\text{RhCp}^*(\text{PMe}_3)(\text{Ph})(\kappa^1\text{-ClCH}_2\text{Cl})][\text{BARF}_4]$,⁶ 2.512(2) \AA , and $[\text{RhCp}^*(\text{PMe}_3)(\text{Me})(\kappa^1\text{-ClCH}_2\text{Cl})][\text{BARF}_4]$, 2.488(1) \AA $\text{Cp}^* = \eta^5\text{-C}_5\text{Me}_5$.⁷ Complex **2** adds to the relatively small number of CH_2Cl_2 complexes that have been crystallographically characterised, and in particular CH_2Cl_2 adducts of pincer, or closely related, complexes.⁸

Although the short Rh–Cl distance might suggest a stronger interaction in **2**, in solution (*vide infra*) rapid exchange between solvent and bound CH_2Cl_2 occurs. The two C–Cl distances in the bound solvent molecule are similar, 1.710(8) [C22–Cl1] and 1.758(7) [C22–Cl2] \AA , although the distal C–Cl bond is the slightly longer of the two. This is in contrast to other reported CH_2Cl_2 complexes in which the bound C–Cl bond is longer.^{8,9} We suggest that the slight lengthening of C22–Cl2 may be due to a number of weak C–H \cdots Cl hydrogen bonds between proximal tBu groups and Cl2.¹⁰

Complex **2** is stable in the solid-state under an Ar atmosphere, and in solution (CD_2Cl_2) for at least 1 week. In the $^{31}\text{P}\{^1\text{H}\}$ NMR spectrum (CD_2Cl_2) a single resonance is observed at δ 204.5 [$J(\text{RhP})$ 136 Hz]. These data are identical to those previously reported by Brookhart and co-workers for the complex tentatively characterised as $[\text{Rh}(\text{tBuPONOP})(\text{CH}_2\text{Cl}_2)][\text{BARF}_4]$, *i.e.* **2**. The tBu groups are observed as a single environment in the ^1H NMR spectrum. The bound CH_2Cl_2 ligand is not observed, even at -80°C in the $^{13}\text{C}\{^1\text{H}\}$ NMR spectrum, presumably as it is undergoing fast exchange with the solvent.¹¹ The electrospray ionisation mass spectrum of **2** using N_2 as a desorption gas showed only **3** as the molecular ion.

Complex **2** is a useful synthon for the preparation of other pincer complexes (Scheme 3). Addition of H_2 to a CD_2Cl_2 solution of **2** forms the previously reported dihydrogen complex $[\text{Rh}(\text{tBuPONOP})(\eta^2\text{-H}_2)][\text{BARF}_4]$ ¹² [$\delta(^1\text{H})$ -8.27 , *lit.* -8.26]. Addition of N_2 forms the new complex $[\text{Rh}(\text{tBuPONOP})(\kappa^1\text{-N}_2)]$ –

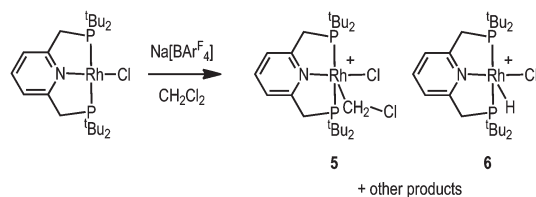


Scheme 3 Reactivity of complex **2**. CH_2Cl_2 solvent. $[\text{BARF}_4]^-$ anions are not shown.

$[\text{BARF}_4]$, **3**, for which a solid-state structure is shown in Fig. 1B. This demonstrates an end-on bound, monomeric, N_2 adduct [N–N, 1.063(5); Rh–N2, 1.967(3) \AA]. The $^{31}\text{P}\{^1\text{H}\}$ NMR spectrum displays a single environment at δ 211.0 [$J(\text{RhP})$ 132 Hz], while in the IR spectrum the N–N stretch is observed at 2201.9 cm^{-1} . The N–N bond length is very similar (albeit a little shorter) than that in free N_2 [1.09 \AA], suggesting only a small degree of activation. Complex **3** can also be compared with previously reported $[\text{Rh}(\text{tBuPnP})(\kappa^1\text{-N}_2)][\text{OTf}]$ which shows a slightly longer N–N bond, a shorter Rh–N bond and a more red-shifted N–N stretch: 1.116(4), 1.898(3) \AA , and 2153 cm^{-1} respectively; suggesting greater N_2 activation for this more electron rich pincer ligand.¹³ This greater metal-based basicity in the tBuPnP complexes is reflected in the CO stretching frequencies of the corresponding CO-adducts: $[\text{Rh}(\text{tBuPONOP})(\text{CO})][\text{BARF}_4]$, **4** [2020 cm^{-1}] and $[\text{Rh}(\text{tBuPnP})(\text{CO})][\text{BARF}_4]$ [1982 cm^{-1}].¹⁴ Complex **4** was prepared by adding CO to a CH_2Cl_2 solution of **2**, further demonstrating the utility of complex **2** in synthesis.

The difference in electron-donating power of the tBuPONOP versus tBuPnP ligands can also be shown by the attempted synthesis of the CH_2Cl_2 adduct of the $[\text{Rh}(\text{tBuPnP})]^+$ fragment, analogous to complex **2**. Rather than simple coordination, this resulted in a number of products as measured by $^{31}\text{P}\{^1\text{H}\}$ NMR spectroscopy. Analysis of single crystals suitable for an X-ray





Scheme 4 Reactivity of $\text{Rh}(\text{tBuPNP})\text{Cl}^{15}$ with $\text{Na}[\text{BarF}_4]$. CH_2Cl_2 solvent. $[\text{BarF}_4]^-$ anions are not shown.

diffraction study, obtained from recrystallisation of the reaction mixture, demonstrated co-crystallisation of two complexes $[\text{Rh}(\text{tBuPNP})(\text{CH}_2\text{Cl})\text{Cl}][\text{BarF}_4]$, **5**, and $[\text{Rh}(\text{tBuPNP})-(\text{H})\text{Cl}][\text{BarF}_4]$, **6**, in an approximate 50:50 ratio (Scheme 4); for which the solid-state structure of **5** is shown in Fig. 1C. Because of this co-crystallisation the metrical data associated with **5** should be treated with caution. The ^1H NMR spectrum of these crystals showed a broad hydride signal at $\delta -15.48$ (relative integral relative to $[\text{BarF}_4]$ of ~ 0.5 H) which is assigned to **6**. Given the number of products formed we are reluctant to speculate on mechanism of formation of **6**, but protonation of **5** by trace acid arising from other decomposition pathways could form **6**. Addition of H_2 to this mixture of **5** and **6** in CD_2Cl_2 afforded mixture of products, from which $[\text{Rh}(\text{tBuPNP})-(\eta^2-\text{H}_2)][\text{BarF}_4]$ could be identified as the major species present.¹⁶

Conclusions

The CH_2Cl_2 complex $[\text{Rh}(\text{tBuPONOP})(\kappa^1-\text{ClCH}_2\text{Cl})][\text{BarF}_4]$ has been isolated, confirming its formation in the decomposition of the corresponding alkane adduct at low temperature, itself formed from protonation of an alkyl precursor.⁴ Synthesis has been achieved by an alternative halide-abstraction route in CH_2Cl_2 solvent, starting from a readily available chloride precursor. This complex, with its weakly bound CH_2Cl_2 ligand, also acts as a useful synthon for other complexes such as N_2 , CO and H_2 adducts. The corresponding PNP ligand complex undergoes C–Cl activation to form a mixture of products, highlighting the difference in electron donating properties of these two ligands.

Acknowledgements

The EPSRC for funding (EP/K035908/1) and Dr Adrian Chaplin for the initial synthesis of complex **5**.

Notes and references

† Crystal data: (2) $\text{RhP}_2\text{O}_2\text{NCl}_2\text{C}_{24}\text{H}_{41}\cdot\text{C}_{32}\text{H}_{12}\text{BF}_2$, Monoclinic ($C2/c$), $a = 16.9996(5)$ Å, $b = 18.1716(4)$ Å, $c = 39.8254(10)$ Å, $\alpha = \gamma = 90^\circ$, $\beta = 96.458(2)^\circ$, volume = $12\,224.4(5)$ Å³, $Z = 8$, $\lambda = 0.71073$ Å, $T = 150(2)$ K, $\mu = 0.53$ mm^{−1}, 16 021 independent reflections [$R(\text{int}) = 0.029$], $R_1 = 0.0814$, $wR_2 = 0.1692$ [$I > 2\sigma(I)$]. CCDC: 1044744; (3): $\text{RhP}_2\text{O}_2\text{N}_3\text{C}_{21}\text{H}_{39}\cdot\text{C}_{32}\text{H}_{12}\text{BF}_2$, Monoclinic ($C2/c$), $a = 16.8578(4)$ Å, $b = 18.1533(3)$ Å, $c = 39.7792(7)$ Å, $\alpha = \gamma = 90^\circ$, $\beta = 95.9972(17)^\circ$, volume = $12\,106.8(4)$ Å³, $Z = 8$, $\lambda = 1.54180$ Å, $T = 150(2)$ K, $\mu = 3.83$ mm^{−1}, 12 215 independent reflections [$R(\text{int}) = 0.031$], $R_1 = 0.0483$, $wR_2 = 0.1183$ [$I > 2\sigma(I)$].

CCDC: 1044745; (5/6) $\text{RhP}_2\text{NCl}_2\text{C}_{24}\text{H}_{45}\cdot\text{C}_{32}\text{H}_{12}\text{BF}_2$: $\text{RhP}_2\text{NCl}_2\text{C}_{23}\text{H}_{44}\cdot\text{C}_{32}\text{H}_{12}\text{BF}_2$, Monoclinic ($P2_1/c$), $a = 13.8327(2)$ Å, $b = 23.4907(3)$ Å, $c = 20.1051(2)$ Å, $\alpha = \gamma = 90^\circ$, $\beta = 97.5982(11)^\circ$, volume = $6475.59(4)$ Å³, $Z = 2$, $\lambda = 1.54180$ Å, $T = 150(2)$ K, $\mu = 4.12$ mm^{−1}, 12 878 independent reflections [$R(\text{int}) = 0.029$], $R_1 = 0.1064$, $wR_2 = 0.2958$ [$I > 2\sigma(I)$]. CCDC: 1044741.

- (a) J. Choi, A. H. Roy MacArthur, M. Brookhart and A. S. Goldman, *Chem. Rev.*, 2011, **111**, 1761–1779; (b) M. C. Haibach, S. Kundu, M. Brookhart and A. S. Goldman, *Acc. Chem. Res.*, 2012, **45**, 947–958.
- (a) *The Chemistry of Pincer Compounds*, ed. D. Morales-Morales and C. M. Jensen, Elsevier, Amsterdam, 2006; (b) *Organometallic Pincer Chemistry*, ed. G. van Koten and D. Milstein, Springer, Heidelberg, 2013.
- (a) B. Rybtchinski and D. Milstein, *Angew. Chem., Int. Ed.*, 1999, **38**, 870–883; (b) N. Selander and K. J. Szabó, *Chem. Rev.*, 2011, **111**, 2048–2076; (c) C. Gunanathan and D. Milstein, *Chem. Rev.*, 2014, **114**, 12024–12087.
- (a) W. H. Bernskoetter, C. K. Schauer, K. I. Goldberg and M. Brookhart, *Science*, 2009, **326**, 553–556; (b) M. D. Walter, P. S. White, C. K. Schauer and M. Brookhart, *J. Am. Chem. Soc.*, 2013, **135**, 15933–15947.
- H. Aneetha, M. Jiménez-Tenorio, M. C. Puerta, P. Valerga and K. Mereiter, *Organometallics*, 2002, **21**, 628–635.
- B. K. Corkey, F. L. Taw, R. G. Bergman and M. Brookhart, *Polyhedron*, 2004, **23**, 2943–2954.
- F. L. Taw, H. Mellows, P. S. White, F. J. Hollander, R. G. Bergman, M. Brookhart and D. M. Heinekey, *J. Am. Chem. Soc.*, 2002, **124**, 5100–5108.
- (a) J. Zhang, K. A. Barakat, T. R. Cundari, T. B. Gunnoe, P. D. Boyle, J. L. Petersen and C. S. Day, *Inorg. Chem.*, 2005, **44**, 8379–8390; (b) A. R. Chianese, M. J. Drance, K. H. Jensen, S. P. McCollom, N. Yusufova, S. E. Shaner, D. Y. Shopov and J. A. Tendler, *Organometallics*, 2014, **33**, 457–464; (c) P. Ren, S. D. Pike, I. Pernik, A. S. Weller and M. C. Willis, *Organometallics*, 2015, **34**, 711–723.
- For example see: (a) J. Schaefer, A. Kraft, S. Reininger, G. Santiso-Quinones, D. Himmel, N. Trapp, U. Gellrich, B. Breit and I. Krossing, *Chem. – Eur. J.*, 2013, **19**, 12468–12485; (b) J. Huhmann-Vincent, B. L. Scott and G. J. Kubas, *J. Am. Chem. Soc.*, 1998, **120**, 6808–6809.
- J. W. Steed and J. L. Atwood, *Supramolecular Chemistry*, John Wiley & Sons, Chichester, 2nd edn, 2009.
- J. Huhmann-Vincent, B. L. Scott and G. J. Kubas, *Inorg. Chem.*, 1999, **38**, 115–124.
- M. Findlater, K. M. Schultz, W. H. Bernskoetter, A. Cartwright-Sykes, D. M. Heinekey and M. Brookhart, *Inorg. Chem.*, 2012, **51**, 4672–4678.
- S. Kloek Hanson, D. M. Heinekey and K. I. Goldberg, *Organometallics*, 2008, **27**, 1454–1463.
- M. Feller, E. Ben-Ari, T. Gupta, L. J. W. Shimon, G. Leituss, Y. Diskin-Posner, L. Weiner and D. Milstein, *Inorg. Chem.*, 2007, **46**, 10479–10490.
- D. Hermann, M. Gandelman, H. Rozenberg, L. J. W. Shimon and D. Milstein, *Organometallics*, 2002, **21**, 812–818.
- A. B. Chaplin and A. S. Weller, *Organometallics*, 2011, **30**, 4466–4469.

